Keck Institute for Space Studies Graduate Fellowship Research Report: High-Resolution Stratigraphy of the Mars North Polar Layered Deposits

Ajay Limaye
California Institute of Technology
Division for Geological and Planetary Sciences
MC 170-25

September 30, 2010

Abstract

The Mars north polar layered deposits (NPLD) consist primarily of water ice and dust, and represent the bulk of the north polar cap [Byrne, 2009]. The NPLD likely hold the most extensive record of recent climate during a period of major insolation variation tied to quasi-periodic orbital changes [Thomas et al., 1992; Laskar et al., 2002]. Data from the High Resolution Imaging Science Experiment (HiRISE) permits definition of layers at sub-meter scale and a renewed analysis of possible orbital expression in NPLD thickness. In this study, image-derived digital elevation models are generated and used to produce thickness measurements in accordance with bed orientation and topographic expression. Stratigraphic columns have been produced for two new sites within the NPLD, and contain several sets of finely bedded units 1-2 m thick; dark, prominent marker beds 3-5 m thick; and undifferentiated units. This work suggests that 1-2 m beds are indeed common in the NPLD; that marker beds are also common, but occur at variable separation distances; and that models of NPLD formation need to incorporate new phenomena to generate the observed scale of bedding. As yet, no distinct orbital fingerprint can be identified.

Introduction

The polar layered deposits (PLD) of Mars hold its richest record of recent climate. Seasonal volatile exchange with the atmosphere causes surface pressure fluctuations of 30 percent, highlighting the continuing interplay between the atmosphere and near-surface ice deposits (Forget, 2004). Radar data reveal typical thicknesses of 1-2 km for both polar caps [Plaut et al., 2007; Phillips et al., 2008]. Thermal emission spectra [Piqueux et al., 2008], rheological [Nye et al., 2000] and thermal models [Mellon, 1996], and density estimates [Zuber et al., 2007] suggest that water comprises most of the polar caps. The PLD also contain dust within and possibly between beds. The relative proportions of H_2O ice, CO_2 ice and dust on the bedding-scale are poorly constrained. Though the time sampled by the PLD is difficult to determine, the PLD likely evolved during a period of major insolation variation due to quasi-periodic evolution of orbital parameters [Byrne, 2009; Laskar et al., 2002]. The PLD have long been expected to hold a record of orbital forcing [Cutts and Lewis, 1982; Thomas et al., 1992], but evidence for this link remains limited.

Dynamical simulations indicate that obliquity has varied from its current 25° by 10° or more over the last several million years, with a period of 120 kyr modulated on 1.2-2.4 Myr timescales [Laskar et al., 2002]. While obliquity alters the annual mean insolation at a given latitude, cycles of precession (51 kyr period) and eccentricity (shortest period ~100 kyr) influence the intensity and duration of seasons. Though on 10 Myr timescales Mars' obliquity is chaotic [Ward, 1973; Laskar et al., 2004], periods of high obliquity prior to 4 Ma would have fostered high sublimation rates at the poles, which may have been sufficient to greatly reduce the

volume of polar ice [Head et al., 2003; Levrard et al., 2007]. Thus the present PLD may largely have responded to the recent (and reasonably constrained) portion of Mars' orbital history.

In the prevailing hypothesis for ice accumulation, atmospheric water condenses upon dust nuclei, which fall to the surface with the addition of condensed CO_2 [Clifford et al., 2000]. The rates of ice accumulation and ablation remain highly uncertain [Laskar et al., 2002; Mischna et al., 2003; Levrard et al., 2007]. Global climate models (GCMs) can address how insolation changes affect transport of water vapor, but long-term dust activity—for example, the frequency of dust storms under different insolation regimes—has proven more difficult to discern. In addition to serving as nucleation agents, dust particles alter atmospheric temperature profiles and can alter PLD albedo, both of which strongly influence the short-term stability of surface ice [Levrard et al., 2007].

Given these complications for modeling PLD formation, an essential task is to characterize the detailed stratigraphic structure of the PLD. Starting with Laskar et al. [2002], several investigators analyzed brightness profiles of the NPLD using Mars Observer Camera (MOC) images and Mars Orbiter Laser Altimeter (MOLA) topographic data, with the aim of capturing periodicity in the stratigraphic record. The consistency of layer thicknesses within a stratigraphic column offers a basic test of orbital control on PLD formation, since periodic climate changes may yield beds of repeating thickness. Power spectra of NPLD brightness derived by [Milkovich and Head, 2005] often showed a peak near 30 m wavelength, but [Perron and Huybers, 2009] found only a ~1.6 m wavelength signal to be significant with respect to a modeled red-noise background common in climate records. Quantitative analysis of PLD stratigraphy using HiRISE imagery and stereo topographic methods now enables stratigraphic analysis at sub-meter resolution. To date, one 400 m section of the upper north PLD has been

characterized at the scale of the finest layering (> 10 cm thickness) [Fishbaugh et al., 2010b]. The authors found several groups of finely layered beds (thicknesses 1-2 m) separated by sequences of darker, prominent "marker beds," named for their relative ease of correlation. Compaction has been hypothesized to modify layer thicknesses, but Fishbaugh et al. (2010b) found little evidence for this process in their 400 m column. This study explores two key aspects of NPLD stratigraphy. The first is to corroborate the limited existing work. Specifically, is the column of Fishbaugh et al. [2010b] characteristic of the meter-scale stratigraphy of the PLD? Fishbaugh and Hvidberg [2006] correlated layered sequences in the upper 500 m of the NPLD using MOC and MOLA data, but work remains to determine whether stratigraphic columns are consistent at the scale of the finest beds. While no direct bed correlations are made herein, the general characteristics of columns are compared.

Second, this study seeks to identify process fingerprints on the distribution of layer thicknesses. As mentioned above, cyclic layer deposition may be recorded in the degree of consistency of bed thicknesses. Moreover, the importance of compaction (a measure of ice material properties) in modifying bed thickness remains an open question, particularly for sections with larger overburden than the site with an existing column.

Methods

With existing datasets, fine layers are definable using image brightness, meter-scale topography, or a combination of the two. Though previous studies of PLD layer thickness have mostly utilized image brightness records, brightness is a property of the surface rather than the bulk layer; thus brightness varies in response to lighting conditions, surface roughness, and the presence of frost or dust veneers [Fishbaugh et al., 2010a; Herkenhoff et al., 2009]. Meter-scale DEMs allow layer definition by breaks in slope in shaded relief maps [Fishbaugh et al., 2010a],

but the topographic irregularity from mantling deposits and erosive processes (including eolian modification, slumping, and sublimation pitting) is similar in magnitude to the stratigraphic thickness of the finest visible layers. Thus the topography may not reveal distinct bedding planes. Since in practice, stripes observed in images are laterally continuous and commonly do correlate with topographic breaks in the co-registered DEM, in this study layers are defined interactively using both image brightness and shaded relief maps.

Layer thicknesses are determined following the techniques of [Lewis et al., 2008]. Analysis begins with DEM generation at 1 m/pixel resolution and ~0.3 m vertical precision. HiRISE stereo pair images are processed using the USGS Integrated Software for Imagers and Spectrometers (ISIS) package and BAE Systems' SOCET SET following methods similar to Kirk et al. [2008]. The elevations of surface points common to each image are defined using individual Mars Orbiter Laser Altimeter (MOLA) retrievals and gridded data. Acceptable DEMs possess residuals—the discrepancy between feature locations and their predicted locations according to the sensor model—with a maximum RMS of ~0.70 m. Subsequently, a terrain extraction routine utilizes a 3x3 pixel search window to correlate features between the images, which limits the DEM resolution to ~ 1 m. DEM quality control entails plotting contours of the extracted topography over the source imagery to assure horizontal and vertical alignment and fidelity to surface morphology. Finally, one HiRISE image is ortho-rectified with respect to the DEM to correct the image for optical distortion.

Using the orthophoto, the orientation of each discernable bed is measured by tracing a profile along the top surface of the bed, interpolating the DEM for elevation along the profile, and determining the best-fit plane using linear regression (Fig. 2). Any solutions for which the uncertainty in the fitted plane's pole orientation exceeds 1° are disregarded. The geometry of

bedding planes is only well-constrained when the exposure is extensive in two dimensions (i.e., curved). When a locale contains fairly consistent bedding orientations, mean strike and dip are utilized to project the elevation of the top of each bed to a common stratigraphic reference frame; a dip correction yields the stratigraphic distance between layers (i.e., layer thickness). Since accurate measurement of bed orientation depends on bed exposure, and bed exposure is often variable, an average strike and dip is inferred for all beds in sections where the measured strike varies by less than 30° and the dip by less than 1°.

Results

As a preliminary test of the measurement techniques, structure and bed thickness were measured for the location described in Fishbaugh et al. [2010b]. Topography has been modeled at five new sites (Fig. 1), based on the availability of overlapping HiRISE observations and the quality of bed exposure. The structure of the Fishbaugh et al. [2010b] site is characterized by shallowly dipping beds (dips generally less than 3°); our measurements yield fairly consistent orientations for adjacent beds (Fig. 2). Nonetheless, subtle orientation differences exist for exposures separated by several hundred meters. Within a section bounded at the top by an unconformity and at the top by layer exposure, the thickness of 23 beds averages 1.7 m with a standard deviation of 0.5 m, consistent with the significant peak in spectral power at ~1.6 m (+-0.1 m) identified by [Perron and Huybers, 2009] for several exposures of NPLD. Fishbaugh et al. [2010b] also noted an average thickness of 1.6 m for the fine beds. New analyses carried out for sites NP4 and NP5 are presented below; analysis of sites NP2, NP3 and NP8 is ongoing.

Site NP4 (Fig. 1 and 3; location 85.1° N, 143.1° E; HiRISE stereo pair PSP_010004_2650/ PSP_010374_2650) occupies a trough wall with a rounded exposure and relief in excess of 1 km. White frost, perhaps seasonal, obscures the highest beds at the site.

Structural measurements indicate the beds lie nearly flat, with an average dip of 0.5°. Three distinct sets of fine beds exist within the measured stratigraphic column (Fig. 3 and 4). The lowermost set begins beneath the starting point of the column, and possesses a stratigraphic thickness greater than 45 m. Some beds of the lower set exhibit local slumping, but most remain intact; however, weathering partially obscures several fine beds at the top of the lowermost set. Moving up the column, the next unit is a dark, topographically prominent marker bed, with some surficial erosional fluting. Undifferentiated (likely post-depositionally smoothed) units then bracket the middle fine layer set, which has a thickness of ~25 m. Two beds above the upper undifferentiated unit are topographically broad, but not as dark as typical marker beds; they are tentatively interpreted as weathered marker beds, although further investigation of their properties across the available section is warranted. Finally, the top thin layer set proceeds upward for ~ 10 m, before terminating in the undifferentiated upper section. As observed by Fishbaugh et al. [2010b], the bed types at site NP4 are sets of fine layers that alternate with thicker, darker "marker" beds. The original morphology of the undifferentiated sections is unknown; they may represent smoothed fine beds, or massive units. Their high degree of young mantling deposits suggests that their current morphology is secondary. Layer thicknesses were directly measured where possible, and compared to relative stratigraphic height within the measured section (Fig. 5). All of the beds measured belonged to fine layer sets. The 12 directly measurable beds all possess thicknesses between 1 and 2 m, and are very similar in thickness to the beds measured at the Fishbaugh, et al. [2010b] site. There is no trend of thinning downward within the section.

Site NP5 (Fig. 6; 84.4 °N, 253.1°E; HiRISE stereo pair PSP_010014_2645/ PSP_010198_2645) occupies a topographically complex region between two local highs. The

local relief is considerably smaller than at site NP4. Small amounts of frost highlight particular layers, but other young mantling deposits roughen bed surfaces. The edges of some units have been blurred to some degree, yet much of the fine layer sets remain remarkably well-defined. The stratigraphic column (Fig. 7) shows that four sets of fine beds are present, the lower two of which are each less than 10 m thick. The lower two fine bed sets are separated by an undifferentiated unit, which nonetheless contains a few faint, continuous horizons that appear to represent mantled fine beds. The upper two sets of fine beds possess similar collective thicknesses (61.7 m for the lower, 58.3 m for the higher). Except for the bottom fine bed set, all fine bed sets are overlain by an undifferentiated unit and then a marker bed. Interestingly, the fine beds once again cluster between 1 and 2 m thickness (Fig. 8), whereas the marker beds appear to form a distinct thickness population (with thicknesses of 3.5 m, 4.9 m, and 3.7 m, from lowest in the section to highest). Once again, there is no indication of thinning within the section, and the measured bed thicknesses are comparable to the corresponding units measured by Fishbaugh et al. [2010b]. The separation distances observed between marker beds (74 m, 67 m), much greater than the 24-36 m separation distance which would correspond to the peak in spectral power at that wavelength noted by [Milkovich and Head 2005] in many sections of the NPLD. Fishbaugh et al. [2010b] note that the 24-36 m separation distance corresponds to only half of the marker beds they observed.

Conclusions

With two completed stratigraphic columns of the north polar layered deposits, this study expands stratigraphic constraints on the recent climate of Mars. The columns presented herein suggest that fine beds of 1-2 m thickness are common, and generally occur in sets of variable number. Given the consistent thickness of individual fine beds across several columns, it

is tempting to infer a quasi-periodic orbital control on bed thickness; yet the inability of current PLD models to tie Mars' orbit to the formation of these thinnest beds remains troubling. Currently, the most advanced GCM-tied model can only produce beds only as thin as 10 m [Levrard et al., 2007]. The time scales and processes involved in making a fine bed sequence remain uncertain. Whereas current models lack a realistic treatment of the activity of broadly distributed shallow subsurface ice at lower latitudes, exploring the implications of this water ice reservoir may prove a fruitful task. In addition to fine beds, marker-type beds are also observed at the new sites; their separation distance does not appear to possess a characteristic value based on existing columns. With current observations, compaction does not appear to play a significant role in modification of NPLD layer thickness at the observed sites, either within individual columns or between columns, as based on the consistent thickness of fine beds. The high variability in marker bed thickness precludes using marker beds to track compaction effects.

Continued work on this project with incorporate observations from sites NP2, NP3, and NP8, as well as examine the ability to correlate sections. Observation areas are limited by the availability of HiRISE stereo image data and by the quality of exposure, but continuing HiRISE observations may reveal additional sites suitable for analysis. Sites NP4 and NP5 occupy similar elevation ranges, as do NP8 and the site analyzed in Fishbaugh et al. [2010b]. The generally shallow dips within the NPLD, as well as the correlative work by Fishbaugh and Hvidberg [2006] with MOC images, suggest that sites at similar elevations may correlate. Continued stratigraphic mapping will provide a valuable reference for modelers of recent Mars climate.

Figures

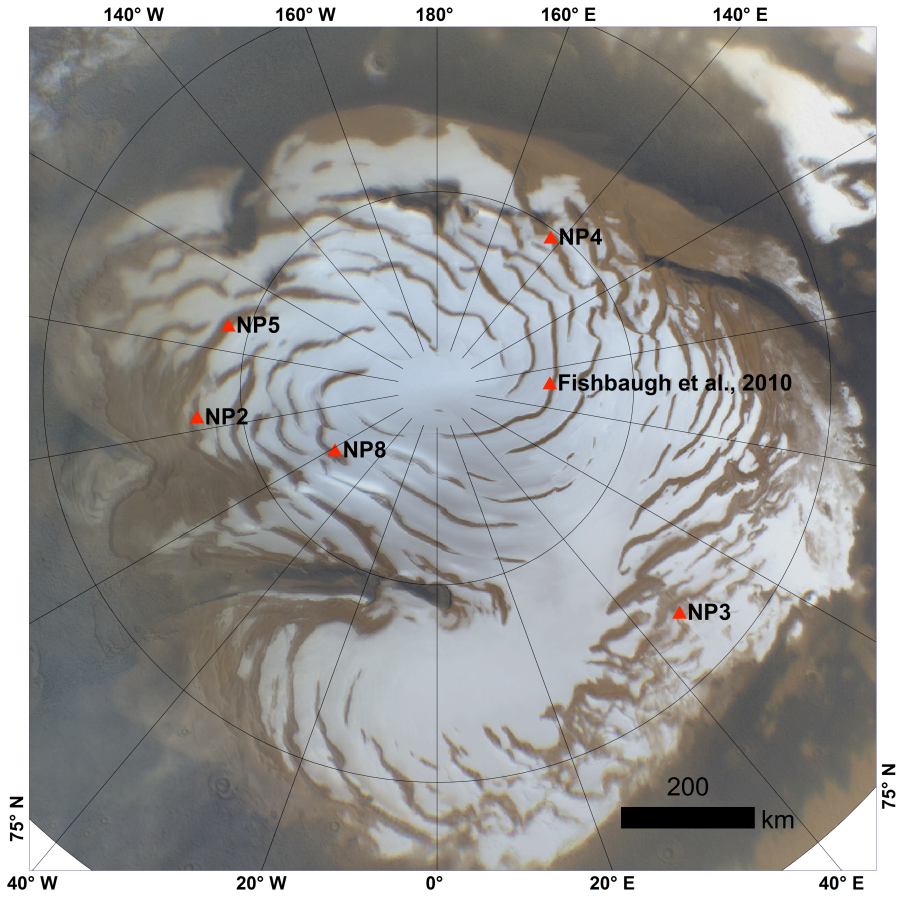

Figure 1. Locations of study sites in the north polar region of Mars. Base image is from the Mars Reconnaissance Orbiter Mars Color Imager (MARCI). Sites under analysis in this study are labeled "NP"; the other site, analyzed in Fishbaugh et al. [2010b], represents the only existing stratigraphic analysis of the north polar layered deposits. Sites NP4 and NP5 are analyzed herein. Digital elevation models have been generated for sites NP2, NP3, and NP8, for which analysis is ongoing.

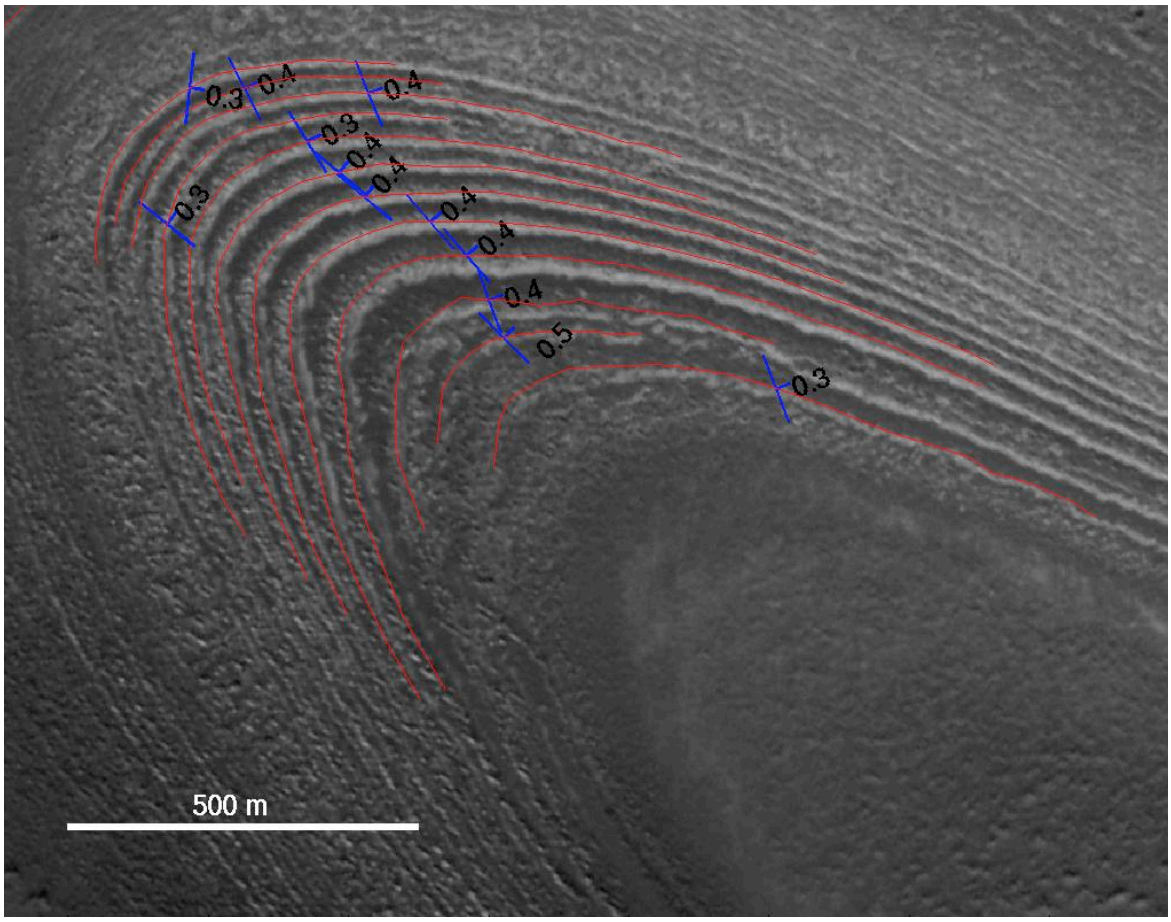

Figure 2**.** Polar layered deposit bedding orientations in a subset of HiRISE image PSP_1738_2670 (centered at 87.1°N, 92.8°E), originally measured by Fishbaugh et al. [2010b]. Strike and dip measurements are based upon best-fit planes corresponding to topographic profiles extracted along red lines.

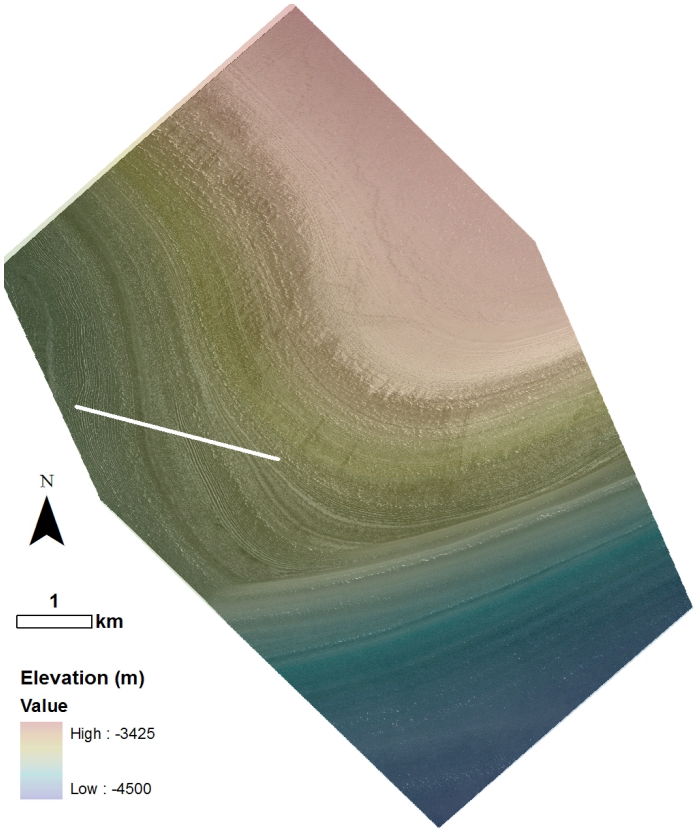

Figure 3. Site NP4. 1 m-resolution digital elevation model derived from HiRISE images, draped over orthophoto of image PSP_010004_2650. White line denotes location of stratigraphic transect; bottom of column in Fig. 4 corresponds to left end of transect.

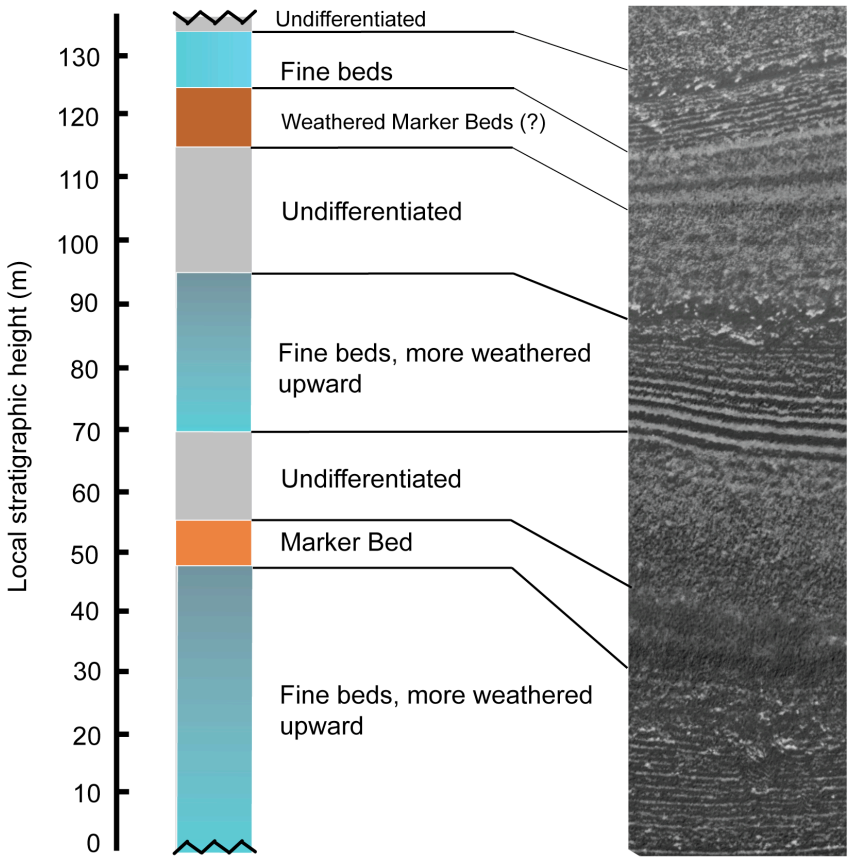

Figure 4. Stratigraphic column of site NP4. Fine bed sequences are colored light blue, undifferentiated sequences gray, and marker beds orange. Darker shades indicate larger degree of weathering. At right, the related portion of orthorectified image PSP_010004_2650. Distance scale in stratigraphic column does not apply to image. Black lines point out contacts.

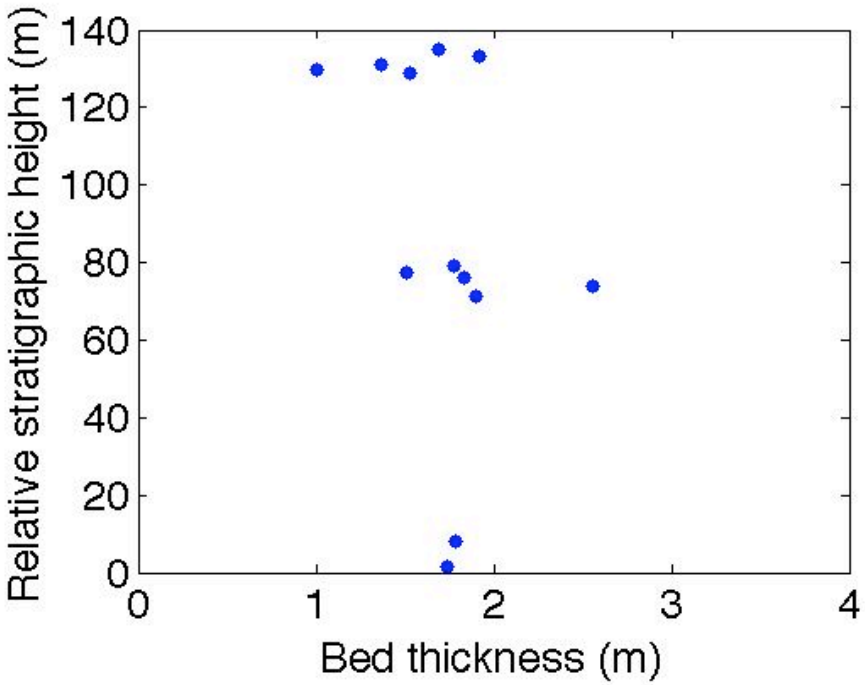

Figure 5. Relative stratigraphic height versus bed thickness for stratigraphic section at site NP4. The number of thickness measurements (n=12) represents the number of directly measured beds; many other beds are present, but are more poorly exposed or more highly eroded.

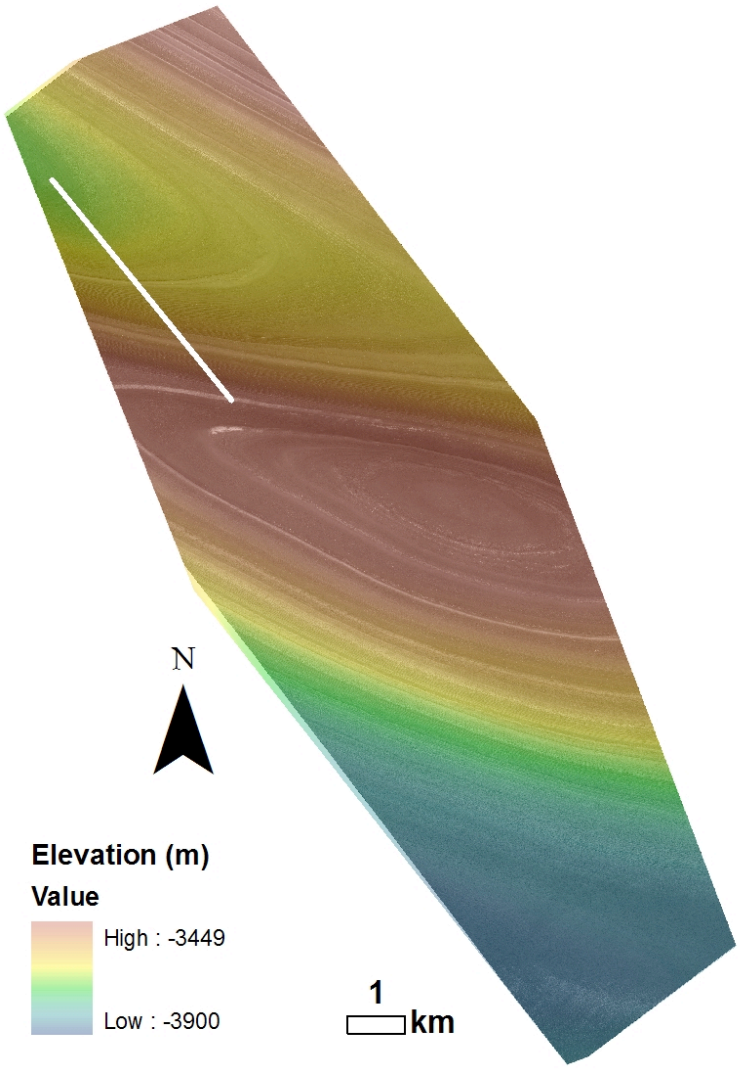

Figure 6. Site NP5. 1 m-resolution digital elevation model derived from HiRISE images is draped over orthophoto of image PSP_010014_2645. White line denotes location of stratigraphic transect; bottom of column in Fig. 7 corresponds to upper left end of transect.

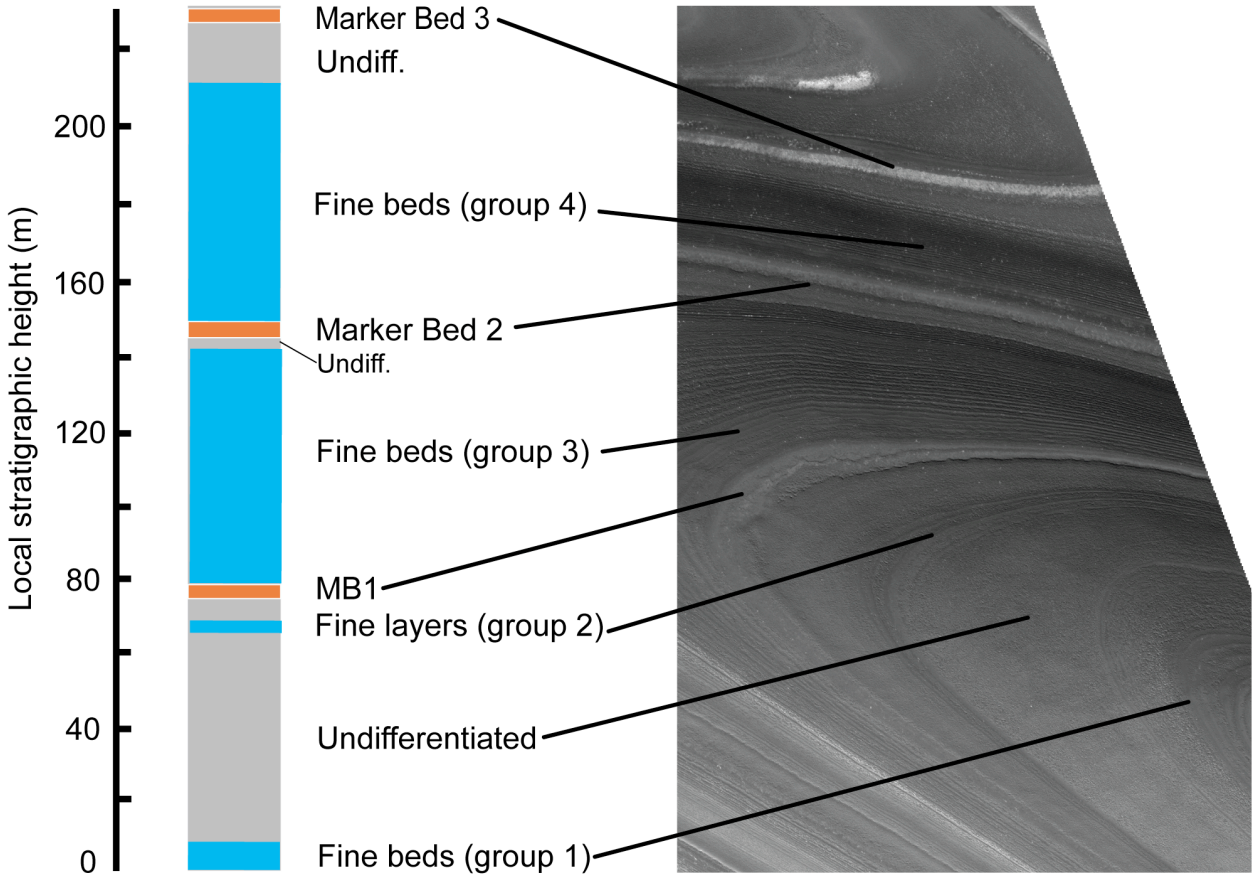

Figure 7. Layer thickness versus relative stratigraphic height for site NP5. Fine bed sequences are colored light blue, undifferentiated sequences gray, and marker beds orange. At right, the related portion of orthorectified image PSP_010004_2650. Distance scale in stratigraphic column does not apply to image. Black lines point out beds (rather than contacts, as in Fig. 3).

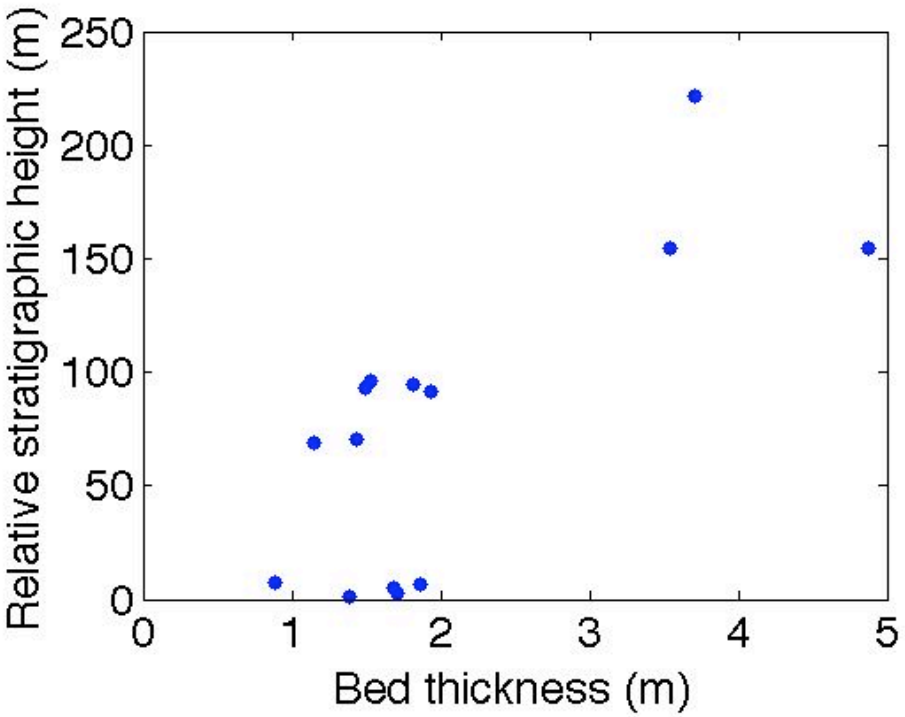

Figure 8. Relative stratigraphic height versus bed thickness for stratigraphic section at site NP4. The number of thickness measurements (n=14) represents the number of directly measured beds; many other beds are present, but are more poorly exposed or more highly eroded. The three beds with thickness greater than 2 m are all marker beds; the rest belong to fine bed units.

Acknowledgements

The W.M. Keck Institute for Space Studies supported this research. Oded Aharonson, Kevin Lewis, and Alex Hayes and Terry-Ann Suer provided advice and training. Thanks to the HiRISE Team for providing image data, and K. Tanaka and C. Fortezzo at the US Geological Survey Astrogeology Team, Flagstaff, AZ, for providing their unconformity map of the north polar region.

References

Byrne, S., 2009, The polar deposits of Mars, Ann. Rev. Earth and Plan. Sci. 37, 535-560.

Clifford, S. M., et al. (2000), The state and future of Mars polar science and exploration, Icarus, 144, 210-242.

Cutts, J. A., and B. H. Lewis (1982), Models of climatic cycles record in Martian polar layered deposits, Icarus, 50, 216-244.

Fishbaugh, K., et al. (2010a), Evaluating the meaning of "layer" in the Martian north polar layered deposits and the impact on the climate connection, Icarus, 205, 269–282, doi:10.1016/j.icarus.2009.04.011.

Fishbaugh, K. E., et al. (2010b), First high-resolution stratigraphic column of the Martian north polar layered deposits, Geophysical Research Letters 37 (L07201), doi:10.1029/2009GL041642.

Forget, F. (2004), Alien weather at the poles of Mars, Science, 306(5700), 1298-1299.

Head, J. W., et al. (2003), Recent ice ages on Mars, Nature, 426, 797-802.

Herkenhoff, K. E., et al. (2009), HiRISE observations of the south polar region of Mars, Lunar and Planetary Science Conference XL.

Kirk, R. L., et al. (2008), Ultrahigh resolution topographic mapping of Mars with MRO HiRISE stereo images: Meter-scale slopes of candidate Phoenix landing sides, Journal of Geophysical Research (Planets), 113(E00A24).

Laskar, J., et al. (2002), Orbital forcing of the martian polar layered deposits, Nature, 419, 375-377.

Laskar, J. et al. (2004), Long term evolution and chaotic diffusion of the insolation quantities of Mars, Icarus 170, 343-364.

Levrard, B., et al. (2007), Recent formation and evolution of northern Martian polar layered deposits as inferred from a Global Climate Model, J. Geoph. Res. (Planets), 112(E06012).

Lewis, K. W., et al. (2008), Quasi-periodic bedding in the sedimentary rock record of Mars, Science 322, 1532-1535.

Mann, M. E., and J. M. Lees (1996), Robust estimation of background noise and signal detection in climatic time series, Climatic Change 33(3), 409-445.

Mellon, M. T. (1996) Limits on the CO_2 content of the martian polar deposits, Icarus 124, 268–279.

Milkovich, S. M., and J. W. Head, III (2005), North polar cap of Mars: Polar layered deposit characterization and identification of a fundamental climate signal, Journal of Geophysical Research, 110(E01005), 21.

Mischna, M. A., et al. (2003), On the orbital forcing of Martian water and CO2 cycles: A general circulation model study with simplified volatile schemes, J. Geoph. Res. (Planets), 108(E6), doi:10.1029/2003JE002051.

Nye J.F., et al. (2000), The instability of a south polar cap on Mars composed of carbon dioxide, Icarus 144, 449–55.

Perron, J. T., and P. Huybers (2009), Is there an orbital signal in the polar layered deposits on Mars?, Geology, 37(2), 155-158.

Phillips, R. J., et al. (2008), Mars North Polar Deposits: Stratigraphy, age, and geodynamical response, Science, 320(5880), 1182-1185.

Piqueux, S., et al. (2008), Distribution of the ices exposed near the south pole of Mars using Thermal Emission Imaging System (THEMIS) temperature measurements, J. Geoph. Res. 113(E08014), doi: 10.1029/2007JE003055.

Plaut, J. J., et al. (2007), Subsurface radar sounding of the South Polar Layered Deposits of Mars, Science, 316(5821), 92-95.

Thomas, P., et al. (1992), Polar deposits of Mars, in Mars, ed. H.H. Kieffer et al., pp. 767-795, U. Arizona Press.

Ward, W. R., (1973) Large-scale variations in the obliquity of Mars, Science, 191(4096), 260-262.

Zuber, M. T., et al. (2007), Density of Mars' South Polar Layered Deposits, Science, 317(5845), 1718-1719.